Population Coding of Self-Motion: Applying Bayesian Analysis to a Population of Visual Interneurons in the Fly

Katja Karmeier,[1] Holger G. Krapp,[2] and Martin Egelhaaf[1]

[1]*Bielefeld University, Lehrstuhl für Neurobiologie, Bielefeld, Germany; and* [2]*Department of Zoology, University of Cambridge, Cambridge, United Kingdom*

Karmeier, Katja, Holger G. Krapp, and Martin Egelhaaf. Population coding of self-motion: applying Bayesian analysis to a population of visual interneurons in the fly. *J Neurophysiol* 94: 2182–2194, 2005. First published May 18, 2005; doi:10.1152/jn.00278.2005. Coding of sensory information often involves the activity of neuronal populations. We demonstrate how the accuracy of a population code depends on integration time, the size of the population, and noise correlation between the participating neurons. The population we study consists of 10 identified visual interneurons in the blowfly *Calliphora vicina* involved in optic flow processing. These neurons are assumed to encode the animal's head or body rotations around horizontal axes by means of graded potential changes. From electrophysiological experiments we obtain parameters for modeling the neurons' responses. From applying a Bayesian analysis on the modeled population response we draw three major conclusions. First, integration of neuronal activities over a time period of only 5 ms after response onset is sufficient to decode accurately the rotation axis. Second, noise correlation between neurons has only little impact on the population's performance. And third, although a population of only two neurons would be sufficient to encode any horizontal rotation axis, the population of 10 vertical system neurons is advantageous if the available integration time is short. For the fly, short integration times to decode neuronal responses are important when controlling rapid flight maneuvers.

INTRODUCTION

Most visual interneurons are sensitive to various stimulus parameters, such as image contrast or the velocity of a stimulus pattern. Hence, the information an individual neuron provides about a stimulus is highly ambiguous. Two additional factors may further increase the ambiguity of a single neuron. First individual neurons are often broadly tuned to a particular stimulus parameter, and two different stimuli may induce the same neuronal response. Second, when stimulated repetitively with the same stimulus, neurons may exhibit a considerable amount of variability that can be due to various sources (e.g., Johnston and Wu 1995). Such ambiguities can be reduced when taking into account the responses of a population of neurons rather than just the response of a single neuron. Indeed, many nervous systems have been concluded to encode information by a distributed pattern of activity spread over a population of neurons (e.g., Georgopoulos et al. 1986; Lee et al. 1998; Nicolelis et al. 1998; Theunissen and Miller 1991; Zhang et al. 1998). Each neuron in the population is tuned to a slightly different aspect of the stimulus. Theoretical studies and model simulations have demonstrated that the accuracy of

population codes depends on the number of neurons constituting the population, the width and form of each neuron's tuning curve, and the variability of the responses (e.g., Abbott and Dayan 1999; Hinton et al. 1986; Pouget et al. 1999; Rolls et al. 1997; Wilke and Eurich 2002; Zohary et al. 1994). Many studies investigate population coding of sensory information by integrating neuronal activities over several hundreds of milliseconds. Biological systems, however, often require behavioral adjustments to take place within considerably smaller time intervals when facing rapid environmental changes (see however Heller et al. 1995; Oram and Perrett 1992; Osborne et al. 2004; Tovee et al. 1993).

To study systematically the impact of integration time on the accuracy of a population code, we combine electrophysiological experiments and numerical modeling. Our experimental system, the blowfly, employs populations of individually identified interneurons processing directional motion information (reviews: Borst and Haag 2002; Egelhaaf et al. 2002, 2005; Hausen and Egelhaaf 1989; Krapp 2000). We focus on a subpopulation of 10 tangential neurons, the vertical system (VS) neurons (Hengstenberg et al. 1982). VS neurons are well described in terms of their response properties (Hengstenberg 1982; Krapp et al. 1998); this makes them an ideal model system to investigate different aspects of population coding. Previous studies suggest that each VS neuron analyzes optic flow resulting from rotations of the animal's head or body around a specific axis located in the horizontal plane (Krapp and Hengstenberg 1996; Krapp et al. 1998). Figure 1*A* shows the receptive field organization of two VS neurons. The preference of a given VS neuron to sense a specific rotation is mediated by the distribution of local directional motion sensitivities within its receptive field. The preferred rotation axes of the VS neurons are distributed within an angular range of ~180° in the horizontal plane (Fig. 1*B*). VS neurons connect either directly or via descending neurons to various motor systems (Gronenberg et al. 1995; Huston and Krapp 2003; Strausfeld et al. 1987). Visual motion stimulation introduces graded membrane potential changes in VS neurons sometimes superimposed by small spike-like depolarizations (Hengstenberg 1977).

In the present account, we make intracellular recordings from VS neurons in a panoramic virtual reality optic flow stimulator (Lindemann et al. 2003). We challenge the neurons with wide-field optic flow stimuli simulating rotations of the fly at two different velocities around different horizontal rotation

---

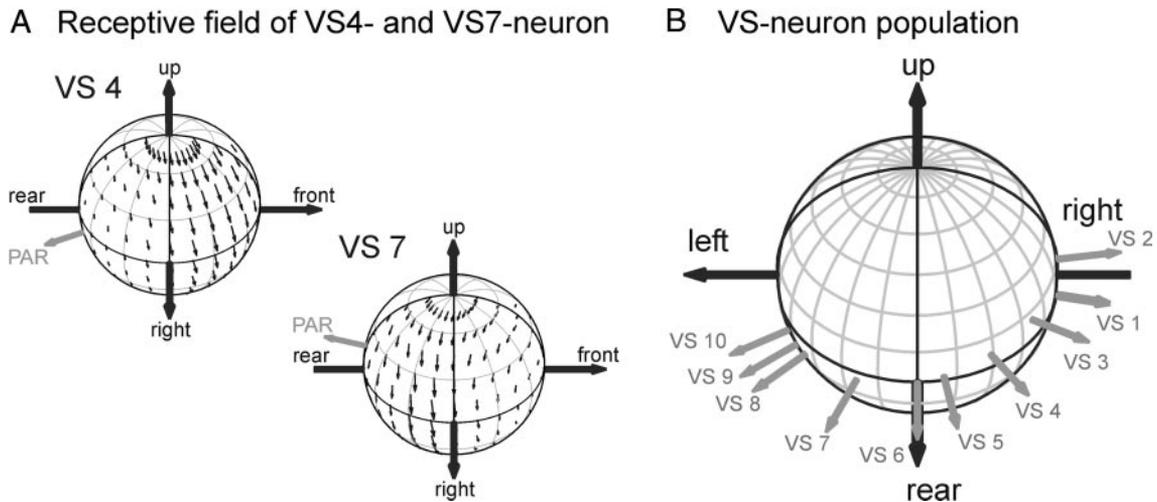## A Receptive field of VS4- and VS7-neuron

B VS-neuron population

FIG. 1. *A*: receptive field organization and preferred rotation axes of the neurons VS4 and VS7 as seen from the right and above. Direction and length of the small arrows in the receptive field indicate the neurons' preferred direction for local motion and motion sensitivities, respectively (data from Krapp et al. 1998). Both receptive fields cover the entire visual hemisphere, but the maximum sensitivity to downward motion is observed in the frontolateral (VS4) and the caudolateral (VS7) visual hemisphere. The preferred axes of rotation (PAR) of VS4 and VS7 differ by ~60°. *B*: preferred rotation axes of all vertical system (VS) neurons in the right brain hemisphere quantitatively estimated from their local response properties (adapted from Krapp 2000) (perspective: from the rear and above). VS neuron responses to wide-field optic flow stimuli simulating horizontal rotations of the fly, are in agreement with the estimated preferred axes shown. Note that the globes in *A* and *B* are rotated by 90° with respect to each other, because the most sensitive regions of the receptive fields are approximately orthogonal to their respective preferred rotation axes.

axes. We chose the velocities to match the lower and upper range of velocities occurring during real flight (van Hateren and Schilstra 1999). On the basis of electrophysiological experiments performed in the present as well as in previous studies (Krapp et al. 1998), we obtain the relevant parameters for modeling the large number of responses that are required to analyze population coding. To find the time interval within which the population activity of VS neurons needs to be integrated for achieving a good estimate of the fly's rotation axis, we apply a Bayesian analysis to the modeled population response. This technique is frequently used in the context of population coding (review: Dayan and Abbott 2001; Oram et al. 1998). A Bayesian analysis determines the coding performance of neuronal populations without referring to a specific neuronal readout mechanism. It only requires the distribution of neuronal responses and the probability distribution of the different stimuli. The Bayesian analysis provides information about the accuracy an ideal readout mechanism could achieve.

By applying this approach, we investigate the accuracy with which the population of VS cells encode the animal's axis of self-motion, depending on integration time, noise correlation among neurons, the distribution of tuning curves, and the number of neurons constituting the population. Apart from the integration time, the noise correlation and the number of neurons in the population are of particular interest to our model system. First double recordings from tangential neurons have indicated that, to some extent, the stochastic membrane potential fluctuations ("noise") in neighboring neurons are correlated (Haag and Borst 2004; Warzecha et al. 1998). Second, 10 VS neurons in each brain hemisphere process rotations around different axes in the horizontal plane. The system seems to be over-determined because, theoretically, no more than two VS neurons should provide sufficient information to estimate any horizontal rotation. We demonstrate that for the given neuronal noise levels, encoding the animal's self-motion within only a few milliseconds requires a population of more than two VS

neurons. The short integration time matches the duration of the fly's alternating self-motion sequences during real flight. (van Hateren and Schiltra 1999).

METHODS

Experiments

ELECTROPHYSIOLOGY. Experiments were done on 1- to 2-day-old female blowflies (*Calliphora vicina*) bred in our laboratory stock. The dissection of the animals for electrophysiological experiments followed standard procedures described elsewhere (see e.g., Warzecha et al. 1993). The flies' eyes were aligned with the stimulus device according to the symmetrical deep pseudopupil (Franceschini 1975). Intracellular recordings from VS neurons in the right lobula plate (3rd optic lobe) were made using borosilicate electrodes (GC100TF10, Clark Electromedical) pulled on a Brown-Flaming Puller (P-97, Sutter Instruments). Electrodes were filled with 1 M KCl and had resistances between 20 and 40 MΩ. Recordings were carried out using standard electrophysiology equipment. The data were low-pass filtered (corner frequency: 2.4 kHz) and sampled at a rate of 4 kHz (I/O-card DT3001, Data Translation) using the VEE Pro 5.0 (Agilent Technologies) in conjunction with DT VPI (Data Translation) software. VS neurons were identified by the location of their receptive field, their preferred direction of motion, and their signal structure (Hengstenberg 1982; Krapp et al. 1998). Experiments were done at temperatures between 28 and 32°C. Such relatively high temperatures closely approximate the fly's head temperature during flight (Stavenga et al. 1993).

VISUAL STIMULATION AND DATA ANALYSIS. Stimuli were presented using *FliMax,* a special-purpose panoramic VGA output device that generates image frames at a frequency of 370 Hz (Lindemann et al. 2003). FliMax is composed of triangle-shaped printed circuit boards (side length: 30 cm), assembled to form 14 of the 20 sides of an icosahedron (radius of inscribed sphere: 22.4 cm). Each of these boards supports 512 regularly spaced round light-emitting diodes (LEDs, Wustlich WU-2-53GD, diameter: 5 mm, emitting wavelength: 567 nm, effective viewing angle 25°). LEDs are controlled individually via a computer equipped with a standard VGA graphics card and customized software. The luminance of each LED is adjustable to

eight intensity levels and is kept constant between updates by sample-and-hold circuits. *FliMax* has an opening in the rear to position a fly in its center and to access the animal's brain for electrophysiological recordings. Due to this opening in the back, neurons with receptive fields mainly located in the posterior part of the visual field (VS9-VS10) (Krapp et al. 1998) were not well stimulated by *FliMax* and are not experimentally analyzed here.

Visual stimuli were designed to simulate optic flow fields resulting from the animal's rotation around various horizontal head axes. A three-dimensional (3D) model of a sphere patterned with randomly distributed black and white patches was designed using Open Inventor (Silicon Graphics). Rotations within this sphere were rendered using Open Inventor and the Mesa (www.mesa3d.org) OpenGL (SGI) implementation (see Lindemann et al. 2003 for details).

We stimulated the fly with optic flow sequences mimicking rotations around 12 different horizontal axes. The different rotation axes were spaced at 30° in the horizontal plane. Each rotation stimulus was presented for 500 ms. Rotations around the fly's longitudinal head axis to the left and right were assigned rotation axes of 0 and 180°, respectively (roll rotation). Nose-down and -up rotations around the transverse head axis corresponded to rotation axes of 90 and 270°, respectively. To obtain the VS neurons' tuning curves, rotations around the 12 axes were presented twice and at two velocities (50 and 3,000°/s). The velocity of the simulated rotation was chosen to match the upper and lower bound the fly encounters during real self-motion as determined by van Hateren and Schilstra (1999). In this study, it was shown that flies exhibit a saccadic flight and gaze strategy. As a consequence, most rotational self-motion components are squeezed into the saccades, leaving mainly translations and only low-velocity rotations for the intersaccadic interval. Therefore we think a simulation of pure self-rotations is adequate. The interstimulus interval was 5 s. To estimate the amount of noise in VS neurons, we presented rotations around a subset of the 12 rotation axes: the fly was either stimulated with rotations around three different axes at both rotation velocities or with rotations around six different axes only at the slow velocity. To obtain as many responses as possible, stimuli were repeated until the recording became unstable. This resulted in 8–14 stimulus repetitions per experiment.

Data were analyzed only if no systematic shift of the resting potential was observed over the entire duration of the experiment and if the excitation level of VS cell's during rotation about its preferred axis exceeded 10 mV. The resting potential before stimulus onset was set to zero in each recording. In some VS neurons, the graded depolarizations of the membrane were superimposed by small spike-like events or spikelets. Neurons with similar response modes have been found in other invertebrate and vertebrate systems (Azouz and Gray 1999; Miller et al. 1991; Sanchez-Vives et al. 2000). Active membrane properties that produce spikelets are particularly pronounced in the VS1 cell (compare VS1 cell and VS2/3 cell in Fig. 2A) (Haag et al. 1997; Hengstenberg 1977, 1982). Because we did not
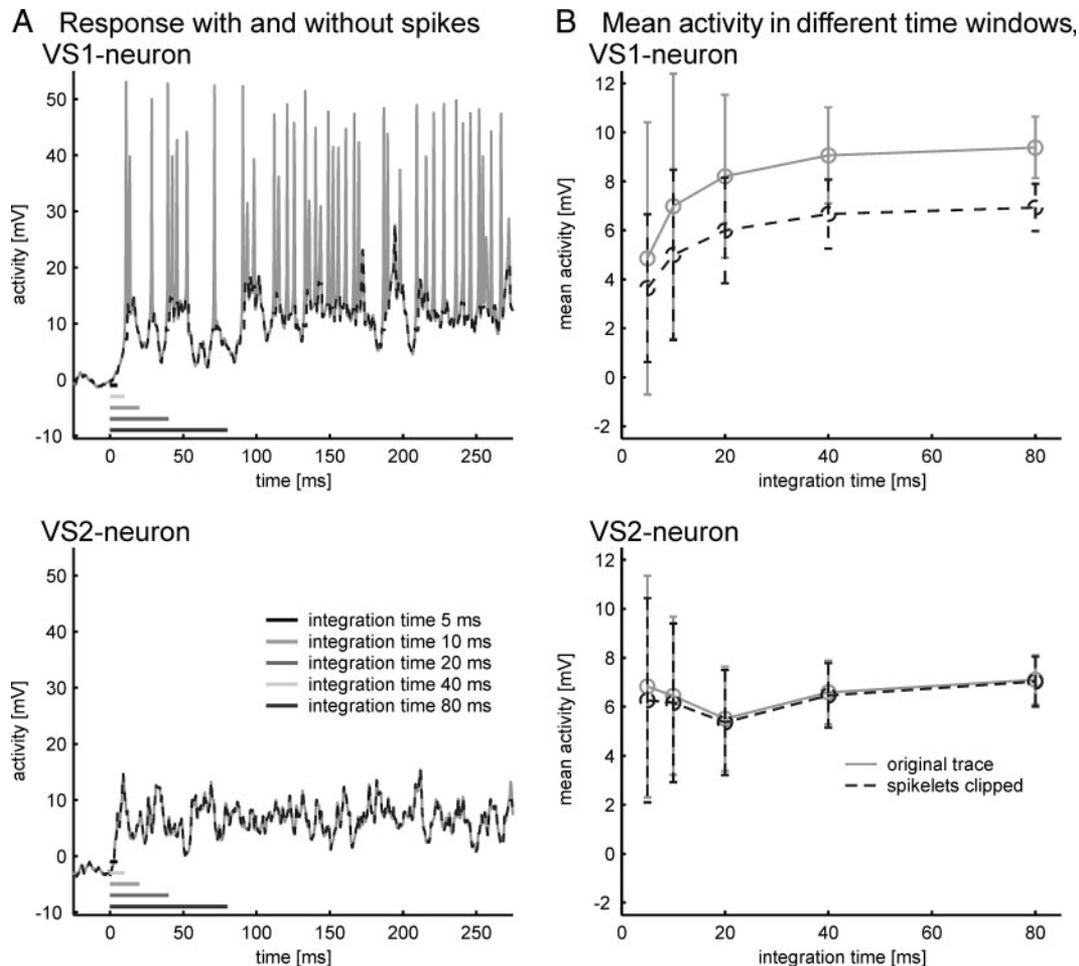

FIG. 2. *A*: single response traces recorded from a VS1- and a VS2/3 neuron. The original traces are shown in black. Gray traces result from clipping spikelets, which are spike-like active events of variable amplitude on top of the graded membrane depolarizations. We stimulated the neurons with optic flow mimicking rotations around axes of 210° (VS1) and 240° azimuth (VS2/3), respectively. Bars above the *x* axis indicate the time windows used to obtain the mean responses shown in *B*. *B*: average responses of the VS1 and the VS2/3 neuron obtained for the time windows indicated in *A*. Means ± SD are shown as obtained from 13 (VS1) and 9 (VS2/3) stimulus repetitions.

want to model this special feature of the VS1 cell in our approximation to population coding in the fly visual system, we decided to clip the spikelets. Clipping the spikelets did not have an impact on our general conclusions (see following text). The spikelets were detected by thresholding the slopes of membrane potential changes. When, due to the occurrence of a spikelet, the slope exceeded a threshold value, they were replaced with the average membrane potential before and after the spikelet. The threshold criterion was defined as 3.5*95th percentile of the slopes in membrane potential changes measured before motion onset. The beginning of a spikelet was defined as the time when the ascending slope of the membrane potential change exceeds the threshold value. The end of a spike was defined when the membrane potential slope drops below this threshold again. The result of this procedure is exemplified in Fig. 2*A* where the original responses and the responses after spike-clipping are shown. The VS1 neuron shows many spikelets during visual activation, whereas the VS2 neuron does not. The consequence of spikelet-clipping on the mean response of these two neurons is shown in Fig. 2*B* for different integration times. The mean activity in the VS1 neuron determined from the neuron's original response trace is 36% higher than the mean activity obtained after clipping the spikelets (average difference: 2 mV). We did not observe any qualitative effects of spikelet clipping on the relationship between mean activity and integration time.

We analyzed in detail the following neuronal response parameters: the time course of the neurons' responses to motion stimuli; the relationship between variance and mean activity; and the orientation of the neurons' preferred rotation axes in the horizontal plane. We define the noise as the variance of the difference between individual response traces and the time-dependent mean response.

Bayesian analysis

To determine the accuracy with which the axis of the animals' self-rotation can be inferred from the population response of VS neurons, we applied a Bayesian analysis (review: Dayan and Abbott 2001; Oram et al. 1998). As a measure of the accuracy, this analysis provides the error with which the axis of the animals′ self-rotation can be decoded from the activity pattern distributed across the population of VS neurons. A Bayesian analysis relies only on estimates of the probability distribution of neuronal activities conditional on an individual stimulus drawn from a given set of stimuli (e.g., Földiak 1993; Salinas and Abbott 1994; Sanger 1996).

The application of a Bayesian analysis to determine the systems accuracy requires the probability distribution of neuronal activities for optic flow stimuli simulating many different rotation axes. Obtaining those probability distributions requires a far greater number of stimulus presentations than could be applied during the limited time available for stable intracellular recordings. To solve this problem, we modeled response traces based on parameters obtained from least-square fits to our experimental data (optimization tool box, Matlab, Mathworks ICN) and on the tuning curves determined in a previous study (Krapp et al. 1998). The details are described in RESULTS. The modeled responses, in turn, were used to approximate the neurons' probability distribution of activities we require for applying the Bayesian analysis.

Many samples of the response r of a neuron to a stimulus s_i allows us to estimate the probability distribution $p(r|s_i)$. The distribution $p(r|s_i)$ describes the probability of observing a certain neuronal response r given that stimulus s_i was presented. Estimating the probability distribution of neuronal responses for all stimuli from the stimulus set $S = \{s_1, s_2, \ldots, s_i\}$ results in the distribution $p(r|s)$. To obtain a measure of the neuronal responses to rotations around a certain axis, we average the neuron's activity within a given time interval. Bayes's rule states that

$$p(s|r) = p(r|s)p(s)/p(r) \qquad (1)$$

where $p(s)$ is the probability distribution of the stimuli and $p(r)$ is calculated as

$$p(r) = \sum_{i=1}^{n} p(r|s_i)p(s_i) \qquad (2)$$

If each stimulus s_i is presented with equal probability, *Eq. 1* simplifies to

$$p(s|r) = p(r|s)/\sum_{i=1}^{n} p(r|s_i) \qquad (3)$$

Once we know the probability distributions $p(s)$, $p(r)$ and $p(r|s)$, which are either set by the experimenter or can be obtained experimentally, we can estimate the probability that a particular stimulus is present given the observed response.

By modeling the activities of all n neurons of a population, we obtain the population response $R = \{r_1, r_2, \ldots, r_n\}$, which allows us to estimate the probability distributions of the population response

$$p(r_1, r_2, \ldots, r_n|s_i) = p(R|s_i)$$

$$p(s|R) = p(R|s)/\sum_{i=1}^{n} p(R|s_i).$$

The distribution $p(R|s)$ contains all information about the stimulus s present in the neuronal population responses. It may be used to compute a stimulus estimate S_{est}. S_{est} is calculated to minimize the variance between the estimated and the true rotation axis by applying the loss-function $L(S, S_{est}) = (S - S_{est})^2$. As a performance measure for estimating the stimulus from the population response, we define the decoding error E, according to a standard procedure as the root-mean-squared difference between the true and the estimated rotation axis (see e.g., Dayan and Abbot 2001). We determined E for rotation axes at a spatial resolution of 1°.

RESULTS

Results of experiments and fitting procedure

TIME COURSE OF RESPONSE. To study the impact of integration time on the accuracy of the population code in VS neurons, we investigate the time course of the stimulus-induced response component for different rotation axes. The stimulus-induced response component is defined as the time-dependent average across the responses to many repetitions of the same stimulus. The time course of the responses was analyzed for intracellular recordings from four different types of VS neurons recorded in six experiments. Each experiment lasted long enough to obtain a sufficient number of response traces required to estimate reliably the response parameters. We stimulated all neurons with slow (50°/s) and fast rotations (3,000°/s) around 12 different horizontal head axes at spacing of 30°. Figure 3*A* (black line) shows the time course of the stimulus-induced responses to a slow rotation around the preferred and the nonpreferred axis. A rotation around its preferred axis maximally activates the neuron. Rotation in the opposite direction ("nonpreferred axis") inhibits the neuron. The time course of the responses to fast and slow rotation velocities differ in amplitude (Fig. 3*B*; see Egelhaaf and Borst 1989; Hausen 1982a,b). For rotations around the preferred axis at both fast and slow velocities the response increases steeply after motion onset. It takes another 20–50 ms for the response to assume a plateau value that stays fairly constant for the remaining
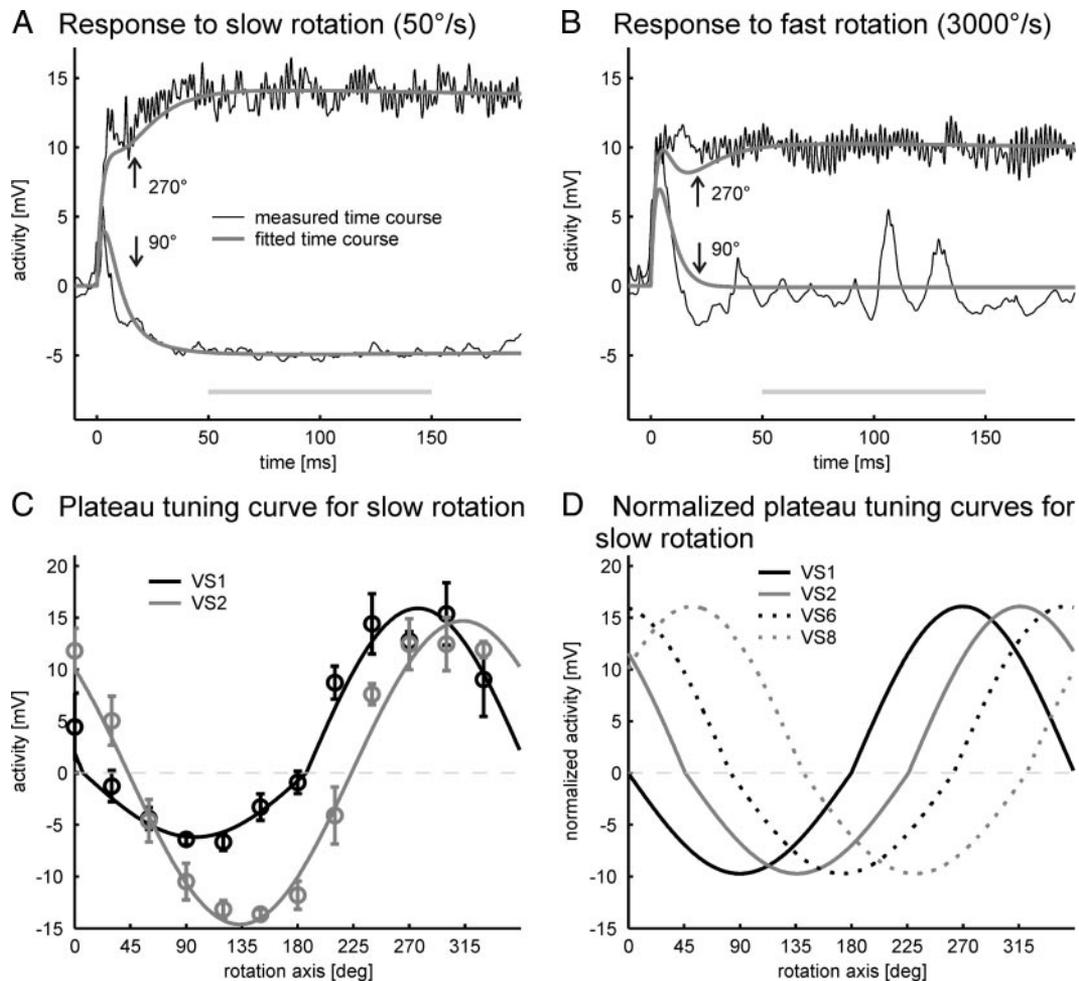
FIG. 3. Experimental results and model fits. *A*: measured stimulus-induced response of a VS1 neuron to a slow rotation at 50°/s around the 270 and 90° axes (black lines). The fit to the time course of the responses is plotted in gray. The stimulus-induced activity is averaged over 2 stimulus repetitions. The bar above the *x* axis indicates the time window used to obtain the plateau values shown in *C*. *B*: measured stimulus-induced response of a VS1 neuron to a fast rotation at 3,000°/s. *C*: plateau tuning curve measured in a VS1 and a VS2/3 neuron. Neurons were stimulated with rotations around 12 different axes at a velocity of 50°/s. Circles give the means ± SD for 2 response repetitions. The plateau value was obtained within a time window of 100 ms length starting 50 ms after response onset. Lines drawn through the measured data indicate a fitted sinusoidal function with different amplitude factors for the positive and negative half-waves. The root of the mean squared error between the fitted and the measured tuning curves amounts to 0.39° (VS1) and 0.27° (VS2/3). *D*: normalized plateau tuning curves to horizontal rotations for all 4 VS neurons recorded in the experiments. The amplitudes were normalized to the mean amplitude obtained from all experiments using slow rotations.

50–500 ms of stimulation (Fig. 3, *A* and *B*). Slow rotations around the nonpreferred axis hyperpolarize the neuron relative to its resting potential. Hyperpolarizations induced during fast rotations are less pronounced. As with responses to preferred axis rotations, a steep transient depolarization precedes the hyperpolarizing plateau value (see also Egelhaaf and Borst 1989). The preferred axis of a given VS neuron does not depend on the rotation velocity.

The limited time of stable intracellular recordings allowed us only to measure VS neuron activities to rotations around 12 different axes. To determine the estimation error *E* for the rotation axes at a much finer spatial resolution, we had to model the time course of responses for those axes we did not obtain experimentally. When modeling the time course of the stimulus-induced response (gray line in Fig. 3, *A* and *B*), we considered two response components: *1*) a band-pass filtered step response starting at response onset that represents the transient depolarization of the response. The peak of the first component proved to be independent of the rotation axis and

was set to 6 and 7 mV for slow and fast rotations, respectively. *2*) A second band-pass filtered step response starting at response onset that accounts for the plateau value of the response. Other than the amplitude of the transient depolarization, the plateau value of the step response depends on the rotation axis.

To obtain the plateau value, we integrated the response within time intervals of 100 ms, starting 50 ms after response onset (see bar in Fig. 3, *A* and *B*). When modeling the first component (*1*) a time constant of 4 ms produced the best fits to the experimental data for both the high- and low-pass filters. For the second component (*2*) best fits were obtained with time constants of 4,950 ms (high-pass) and 15 ms (low-pass). The only parameter for modeling the time course of the response that depends on the rotation axis is the plateau value of the second response component. Fitting a function to the plateau values of the responses measured at 12 rotation axes allowed us to derive the plateau values of the responses to intermediate rotation axes. We will refer in the following to the function

fitted through the measured plateau values as plateau tuning curve. The plateau tuning curves can be approximated by phase-shifted cosine functions using different amplitude factors for the positive and the negative half-wave. The amplitude factors are different for slow and fast rotations. In Fig. 3C, we plot the experimentally determined plateau values of two different VS neurons to slow rotations together with the corresponding plateau tuning curves. Plateau tuning curves of a given VS neuron obtained in different flies were found to be very similar (maximal shift of the preferred rotation axes: 14°). The mean amplitude factors and SDs of the positive (negative) half-wave of the plateau tuning curves were 15,45 ± 1,18 mV (−9,74 ± 4,08 mV) for slow and 7,54 ± 2,77 mV (−2,23 ± 4,14 mV) for fast rotations as averaged across all experiments. The positive amplitude factors of all plateau tuning curves were normalized to the mean obtained from six experiments. The negative amplitude factors were normalized correspondingly. Figure 3D shows the normalized plateau tuning curves of four different VS neurons. The preferred axes of rotation and the overall form of the tuning of all VS neurons as obtained with global optic flow stimuli are in close agreement with predictions based on local motion stimuli (cf. Fig. 1B) (Krapp et al. 1998; see Karmeier et al. 2003 for further details on the prediction of the preferred rotation axis from the neurons' receptive field organization). Therefore instead of determining experimentally the time course of responses for all 10 VS neurons, for the remaining six VS neurons, we calculated the time course based on the neurons' receptive field organization.

Noise

The membrane potential of individual response traces of VS cells fluctuates considerably about the stimulus-induced response component, i.e., the mean across the responses to many stimulus repetitions (see METHODS and preceding text). Despite these stochastic membrane potential fluctuations, the variability of the responses of fly tangential neurons to repeated presentation of the same stimulus is much smaller than the

variability of vertebrate cortical neurons (Barberini et al. 2001; Warzecha and Egelhaaf 2001). The fluctuations were still conspicuous even after the spikelets had been removed. The stochastic component of the membrane potential is determined by subtracting the stimulus-induced response component from an individual response. Figure 4A shows the probability distribution of the stochastic membrane potential component obtained in the plateau phase within a 400-ms time window that starts 100 ms after motion onset. This distribution may be approximated by a normal distribution. Figure 4B shows the variance of the stochastic membrane potential component as a function of the mean stimulus-induced component for both fast and slow rotation velocities. The variance increases with increasing stimulus-induced depolarization of the cell, reaches a maximum and, for even higher activity levels, decreases again. Because the mean stimulus-induced activity varies during the initial response phase after motion onset (cf. Fig. 3, A and B), we averaged the stimulus induced activity within 50-ms time windows overlapping by 25 ms. The resulting mean activities were assigned to 0.5-mV activity classes. The dependence of the variance on the mean activity does not depend critically on either the length or the overlap of the chosen time windows and can be fitted by a Gaussian function (Fig. 4B; $\sigma = 5.2$, $\mu = 7.5$, max. amplitude: 10.1).

Population coding of self-motion

MODELING RESPONSES FOR THE BAYESIAN ANALYSIS. To apply the Bayesian approach based on our experimental data, we modeled the time course of VS neuron responses and their noise statistics. Neuronal responses of all 10 VS neurons located in the right brain hemisphere were modeled at a temporal resolution of 1 ms and a spatial resolution of the rotation axis of 1°. The mean time course of each neuron's membrane potential $r(t)$ for a given rotation axis is composed of the transient depolarization and the plateau value, scaled to the value of the plateau tuning curve (see RESULTS OF EXPERIMENTS AND FITTING PROCEDURE).
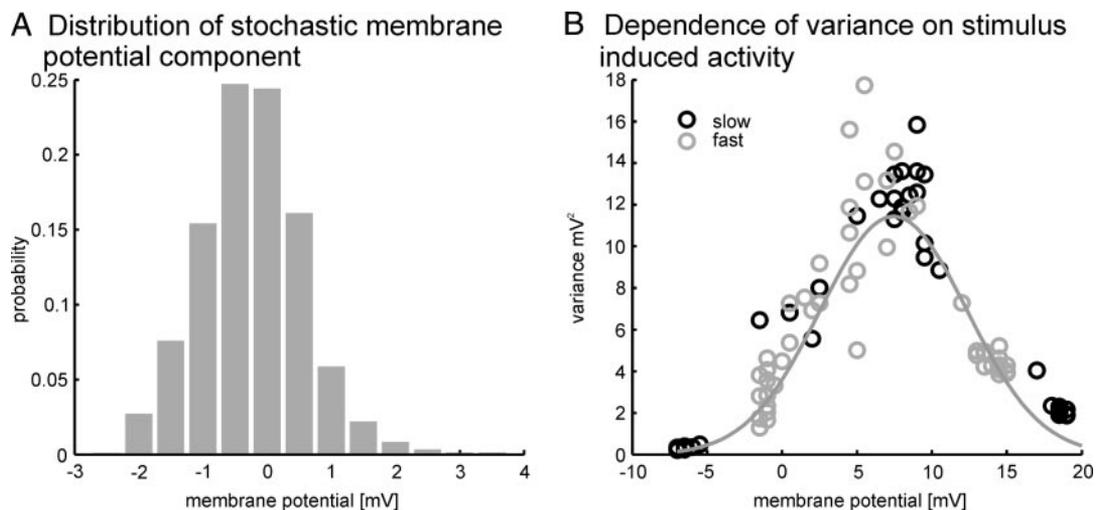

A Distribution of stochastic membrane potential component

B Dependence of variance on stimulus induced activity

FIG. 4. A: probability distribution of the stochastic membrane potential component for 9 stimulus repetitions (slow rotations around the 270° axis). The time interval used for analyzing the membrane potential starts 100 ms after stimulus onset and lasts for 400 ms. B: the variance of the stochastic membrane potential component scales nonlinearly with the stimulus induced membrane potential component. The variance of the stochastic membrane potential component is analyzed for 3 different rotation axes and both rotation velocities. Each stimulus was repeated ≥8 times. The variance and mean of each response trace are analyzed in 16 time windows of 50-ms length, overlapping by 25 ms. We determined the dependence of the variance on the membrane potential in three experiments. The data shown are obtained from the same VS1 recording as used for Fig. 3, A and B.
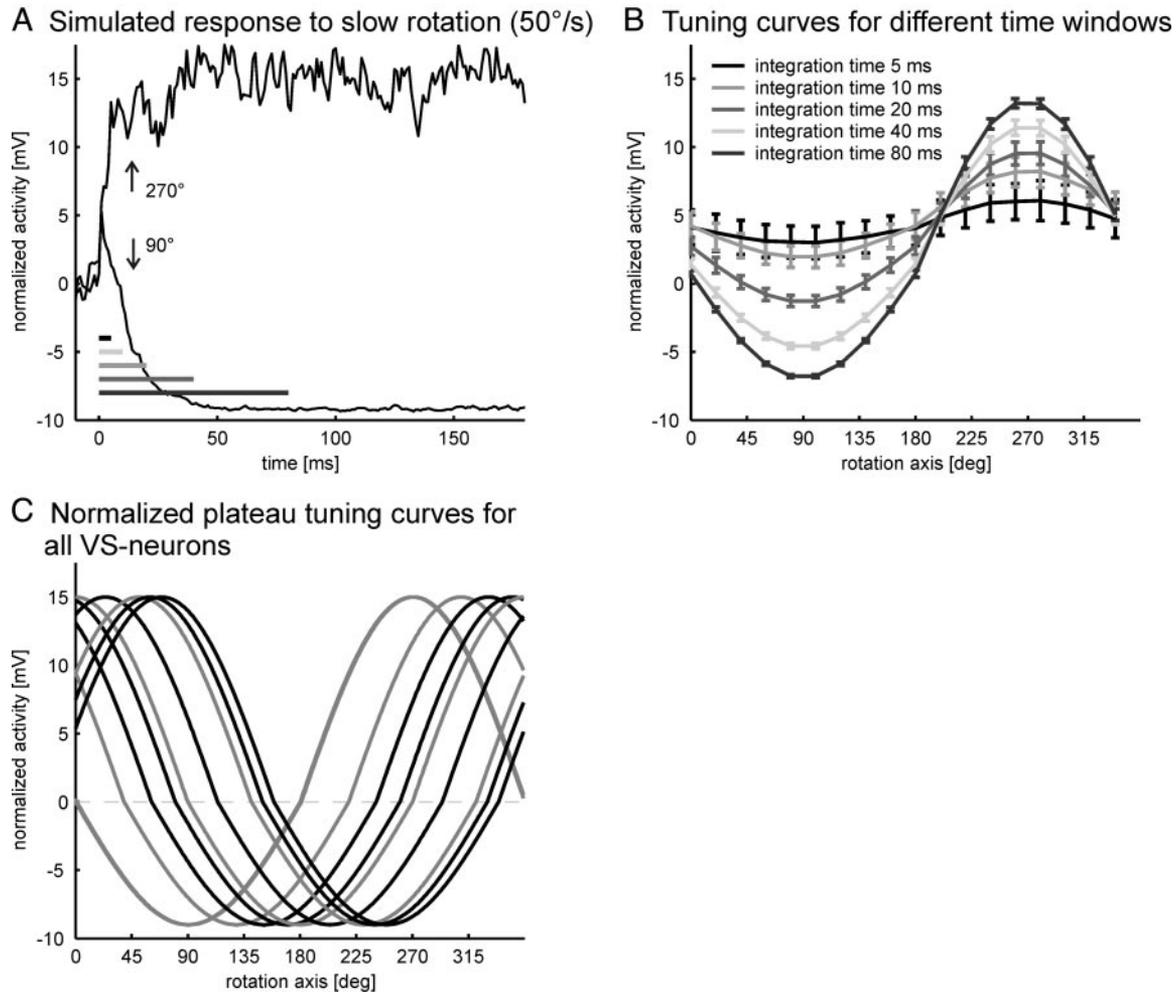
A Simulated response to slow rotation (50°/s)

B Tuning curves for different time windows

C Normalized plateau tuning curves for all VS-neurons

FIG. 5. Modeling approach. *A*: simulated VS1 response trace to a slow rotation around the 270 and 90° axes. Bars above the *x* axis indicate the integration windows used in the further analysis. *B*: tuning of the VS1 neuron calculated from average responses in the different time windows plotted in *A*. Bars give the SD. *C*: normalized plateau tuning curves for slow rotations of all 10 modeled VS neurons located in the right brain-hemisphere. Tuning curves of the neurons that were not only modeled, but also recorded in the experiments are given in gray (cf. Fig. 3*D*). The tuning shape and the preferred axis of rotation determined for the VS neuron with wide-field optic flow are in close agreement with predictions based on local motion stimuli.

Each individual response trace $r_i(t)$ was computed by adding individual noise traces $n_i(t)$ to the mean time course of the membrane potential $r(t)$

$$r_i(t) = r(t) + n_i(t)$$

Individual noise traces were computed as a series of low-pass-filtered random numbers drawn from a Gaussian distribution (for further details see: Kretzberg et al. 2001). The noise is scaled according to its dependence on the mean activity as derived from our experimental data (Fig. 4*B*).

Figure 5*A* shows an individual model response of a VS1 neuron. The time course of the modeled responses nicely captures the features of our experimental data (compare Figs. 3*A* and 5*A*). From the repeated calculation of individual responses to different rotation axes, we obtained the distribution of neuronal activities conditional on each stimulus $p(r|s)$. The activities were integrated over time windows of 5-, 10-, 20-, 40-, and 80-ms length. The conditional probability distributions allowed us to reconstruct the mean tuning curves and SD for different time windows (Fig. 5*B*). Modeling the activities of all 10 VS neurons of the population allows us to estimate the probability distributions of the population response for 360

rotation axes (spatial resolution: 1°). Figure 5*C* shows the normalized plateau tuning curves for all 10 VS neurons of the right brain hemisphere. We compute the decoding error as described in METHODS (Fig. 6*A*).

Accuracy of VS system

We estimated how accurately horizontal rotations of the animal could be decoded from the activity pattern within the population of 10 VS neurons located in one brain-hemisphere. The mean responses of each neuron of the population were calculated from individual response traces in time windows of 5, 10, 20, 40, and 80 ms after response onset (Fig. 5*B*). In Fig. 6*A*, we plot the error *E* obtained from the population response. The error slightly depends on the rotation axis. A rotation around an axis at an azimuth of 360°, for instance, is encoded more accurately than a rotation around an axis at 180° azimuth (Fig. 6*A*, black line). With increasing integration time the decoding error decreases. A decrease of the error for longer integration times is expected for two reasons: the increasing modulation depth of the tuning curves (Fig. 5*B*) and the decrease of the SD of the noise (error bars in Fig. 5*B*). Due to

A Error

B Error for slow and fast rotation

C Correlation between VS-cells
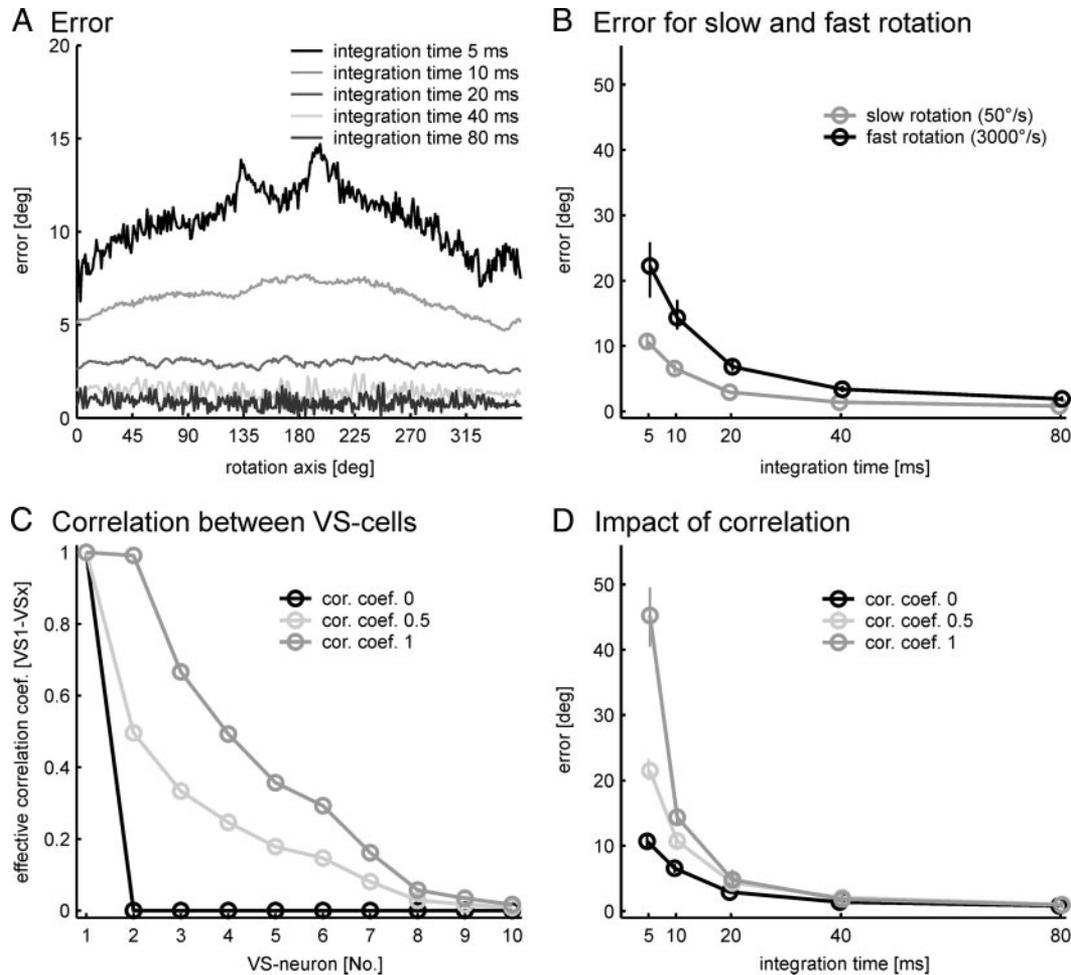

D Impact of correlation

FIG. 6. Error for slow and fast rotations and effect of correlated variability. *A*: decoding error for the population of VS neurons as a function of the rotation axis (slow rotation; 50°/s). We compute the error from repeatedly modeled responses of all 10 VS neurons. The gray-scale code indicating the 5 integration windows is the same in Fig. 5. *B*: error as a function of the integration window starting at response onset for slow and fast rotations with uncorrelated noise. Solid lines give the median error over all rotation axes, bars indicate the 25th and 75th percentile for each integration window. *C*: correlation coefficient effective between the VS1 neuron and all other VS neurons. The correlation coefficient given in the legend applies to 2 neurons with completely overlapping receptive fields. *D*: error for slow rotations without correlated noise and with a correlation coefficient of 0.5 or 1 for a neuronal population with identical tuning curves.

the specific time course of the responses, the tuning curves reconstructed from the modeled responses for short integration times modulate only slightly with changes in the rotation axis. This is a consequence of the transient depolarizations after stimulus onset, a common feature of the responses to any rotation axis. Consequently, the decoding error is relatively large for short integration times. As an overall measure of accuracy for a given time window we apply the median across the error for all rotation axes. For slow rotations, the median error drops <7° already after an integration time of only 10 ms (Fig. 6*B*). The error bars in Fig. 6*B* indicate the 25th and 75th percentile and reflect the modulation of the error across all rotation axes. The system's accuracy decreases for simulated rotations of 3,000°/s. But even for fast rotations the median error drops <15° after an integration time of 10 ms (Fig. 6*B*).

Correlation of noise

The results presented so far were calculated for a population of neurons with uncorrelated noise, i.e., the time course of stochastic response components were statistically independent between the neurons. However, the receptive fields of most VS

neurons overlap (cf. Fig. 1*A*), and it is assumed that they partly receive input from the same presynaptic elements. Dual recordings from two spiking tangential neurons with largely overlapping receptive fields revealed that in these neurons 30% of the spikes are generated synchronously (Warzecha et al. 1998). Moreover, a recent study indicates that neighboring VS neurons are directly coupled via electrical synapses (Farrow et al. 2005; Haag and Borst 2004). This would certainly increase the noise correlation between VS neurons. In agreement with these experimental findings, we included correlated noise in our simulations. We assumed that the noise between VS neurons is positively correlated to a degree that depends on the overlap of their receptive fields and thus on the separation of the neurons' preferred rotation axes.

Accordingly, two (hypothetical) neurons with identical preferred rotation axes have the strongest noise correlation. The correlation coefficients assumed for neurons with identical preferred rotation axes were 0, 0.5, or 1 (Fig. 6*C*). If the preferred axes differ from one another, the correlation coefficient is scaled down by a factor that is computed as the tuning curves' area of overlap normalized to the area of the entire

tuning curve. Tuning curves of the modeled VS neuron population never completely overlap, and the correlation coefficient between two neurons is thus always smaller than the coefficient assumed for neurons with identical preferred axes (Fig. 6*C*). If we assume a correlation coefficient of 0.5 for neurons with identical preferred rotation axes, the noise between the VS1 neuron and the VS2 neuron is correlated with a coefficient of 0.49 (pale gray curve in Fig. 6*C*). In this case, 49% of the noise originates from the common input of the neurons, and 51% is intrinsically generated and/or originates from inputs the neurons do not share. We model the noise traces of these two neurons by adding two components: One component is the same for both neurons and is scaled to a variance of 0.49 mV^2. The other component contains independent noise and is scaled to 0.51 mV^2.

Noise correlations of all tested strengths decrease the accuracy of the VS-neuron population, particularly for short integration times (Fig. 6*D*). However, even for maximally correlated noise the decoding errors drop <5° within 40 ms after response onset. By that time, the negative effect of correlated noise seems to be functionally negligible.

Number of neurons

In a noise-free system, two neurons with orthogonally arranged preferred axes are sufficient to encode any horizontal rotation. To assess the potential significance of 10 rather than 2 VS neurons, we compute the decoding error for a hypothetical population of two VS neurons whose preferred axes are arranged in an orthogonal way (gray tuning curves in Fig. 7*A*). Otherwise, we assume the same time course of the responses and the same variance as measured in VS neurons and no noise correlation.

The simulations show that, for short integration times, two neurons cannot estimate the rotation axis as accurately as the population of 10 neurons and that the encoding error is larger by a factor of >3–5 (cf. Figs. 6*B* and 7*B*). Nevertheless, a detection of the rotation axis with a median error of 7° is achieved for integration times as short as 20 ms (Fig. 7*B,* gray line). The comparatively high performance of a population of only two neurons is due to the graded response mode of VS neurons. If we approximate crudely two spiking neurons by rectifying the tuning curves, only after integration times of >40 ms, the decoding error drops <10° (Fig. 7*B,* dotted line). Furthermore, the error is strongly modulated and depends critically on the respective rotation axis (Fig. 7*B,* inset). Even if the median error drops <5° after 80 ms, for some rotation axes the error is as high as 45°!

The accuracy of the neuronal population coding information with graded membrane potential changes improves if the integration window does not start directly at response onset but 100 ms later (Fig. 8). The higher accuracy for later time windows can be attributed to two factors. First, the initial transient response of VS neurons is less dependent on the rotation axis than the plateau response (see Fig. 3*A* and *B*). Second, the population response is less variable due to the dependence of the variance on the mean response (see Fig. 4*B*). During the plateau response, two neurons determine the rotation axis at high accuracy already within 1 ms, even in the presence of noise (median decoding error: 4.3°). For a smaller population of VS cells and given the specific time course of the
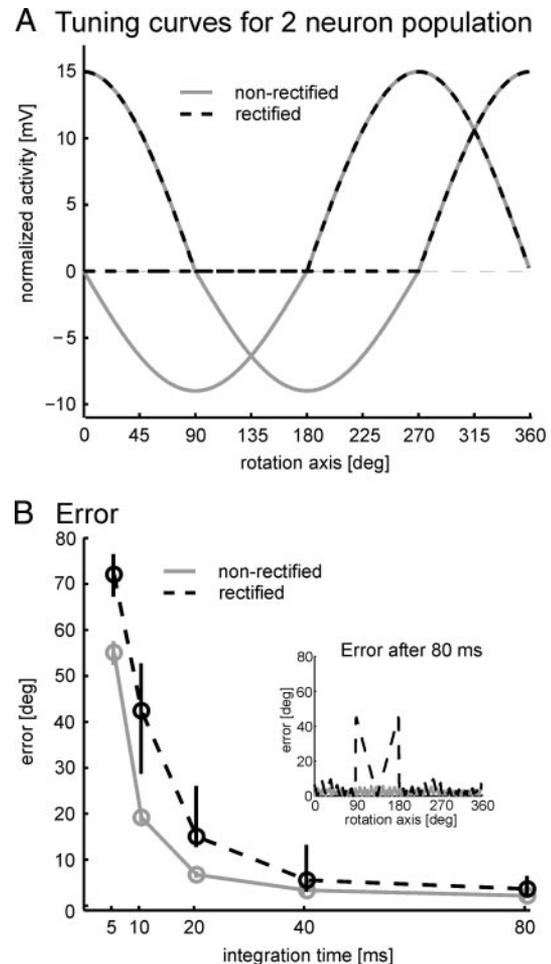

FIG. 7. Decoding the rotation axis from the population response of 2 neurons. *A*: tuning curves for 2 neurons with a graded response mode (nonrectified, gey lines) and with a rectified tuning curve mimicking the spike rate of a spiking neurons (dashed lines). *B*: decoding error as a function of integration time for neurons with rectified and nonrectified tuning curves. Even if the median error for the spiking neurons after 80 ms integration time is in the same range as for the neurons with a graded response mode, some rotation axes can only be reconstructed with a low accuracy (*inset*).

VS neuron responses, an accurate estimation of the rotation axis requires either sufficient integration time or it requires the integration to start some time after response onset. These decoding strategies, however, are not particularly advisable if the transitions between different self-motions take place very rapidly as they do in flies (Schilstra and van Hateren 1999). A fast and accurate estimation of the rotation axis under dynamical stimulus conditions, therefore requires a larger population of neurons than the minimum number of two.

Spatial distribution of neurons

The preferred axes of the ten VS neurons as determined experimentally (Krapp et al. 1998) are not equally spaced along the azimuth (Fig. 5*A*). To test the impact of the spatial arrangement of the preferred rotation axis on the decoding error, we investigate three different situations. *1*) The preferred axes of the 10 VS neurons are equally spaced within an azimuth range between 81 and 270°, which corresponds to the range within which the experimentally determined axes were

A Time windows

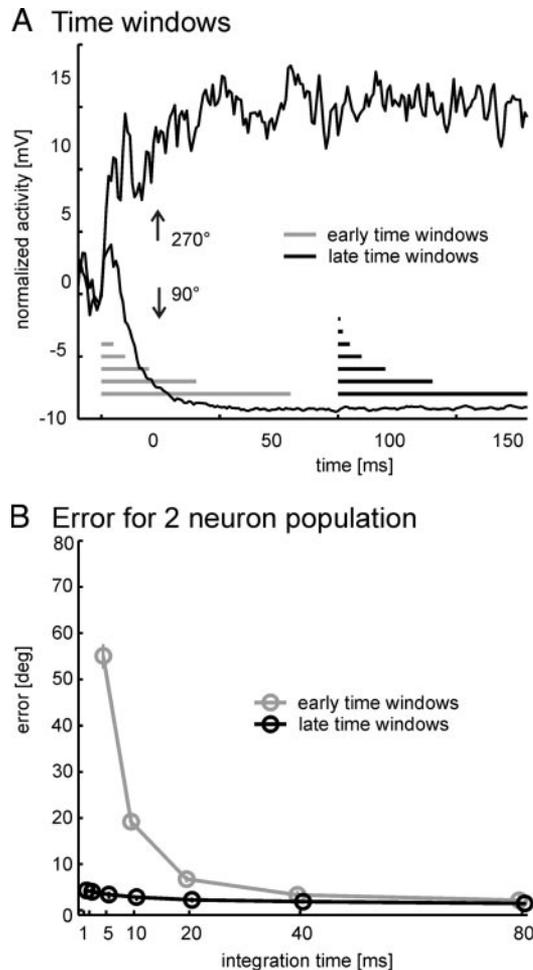
B Error for 2 neuron population

FIG. 8. Coding accuracy of a 2-neuron population for 2 different starting times of the integration window. Neurons are arranged as shown in Fig. 7A. A: responses traces for rotations around axes at 0 and 180°; the preferred rotation axis is at 0°. Bars below the traces indicate the integration windows starting directly at response onset (gray) or 100 ms later (black). B: decoding error as function of integration time for windows starting at response onset or 100 ms later.

found. 2) The preferred axes of 3, 4, and 3 neurons cluster around 270, 0, and 60° azimuth. 3) The preferred axes of 3, 4, and 3 neurons coincide at 270, 0, and 60° azimuth. In Fig. 9A, we plot the tuning curves for the different spatial arrangements. The coding accuracy is computed from 10 ms integration windows starting at response onset.

In the case of uncorrelated and medium correlated noise, the specific arrangement of the preferred axes does not affect the median error (Fig. 9B). Only for the highest noise correlation, the error increases and the arrangement of the preferred axes has a small effect. However, even for this correlation the mean error of the population with three clusters of completely overlapping tuning curves (3) is only 2.3° higher than for the population with equally distributed tuning curves (1). For a population of broadly tuned VS neurons in graded response mode the exact spatial arrangement of the neurons can thus be neglected.

DISCUSSION

In this study, we combined experimental data and modeling to investigate the accuracy of a population code. Population responses were modeled to fit electrophysiological data recorded from VS neurons in the fly visual system on wide-field optic flow stimulation. We demonstrate that the population of VS neurons encodes any horizontal rotation axis with a reasonable error within the very short time interval of 10 ms. When applying a Bayesian analysis to compute the accuracy of a population code, we obtain an upper bound of a system's theoretical coding accuracy. This method, however, does not allow us to infer how the decoding of sensory information is accomplished in a particular neuronal system. So far, little is known about which components of the signals carried by VS neurons are decoded by subsequent processing stages and used for motor control (e.g., Gronenberg et al. 1995; Huston and Krapp 2003; Strausfeld et al. 1987). Nevertheless, the factors that affect the coding accuracy of a neuronal population code can be pin-pointed by a Bayesian analysis. In the following, we will discuss three of these factors: the integration time, noise correlation between neurons, and the population size and spatial arrangement of neurons.

Integration time

The population of VS neurons encodes the rotation axis for slow rotations with a median error of 7° after an integration time of only 10 ms starting at response onset. Extending the integration time to >20 ms only results in minor improvements. The accuracy of the population code decreases at high rotation velocities of 3,000°/s. However, after an integration time of 20 ms even at this velocity a decoding of the rotation axis is possible with an acceptable accuracy (median error: 7°). Interestingly, the shortest integration times that are sufficient to decode the population activity of VS neurons with a high accuracy are smaller than the time constants and integration times of the motion detection mechanism presynaptic to VS neurons (e.g., Borst et al. 2003; Egelhaaf and Borst 1989; Lindemann et al. 2005; Srinivasan 1983).

Averaging neuronal responses over time reduces neuronal noise and can enhance the accuracy of a population code. For neurons that do not immediately reach their steady-state response, as was the case for the VS neurons in our experiments, increasing the integration time has another positive effect. Because the neuronal response starts with a depolarizing onset peak that is independent of stimulus direction, integration over time increases the neuron's specificity to a certain stimulus (cf. Fig. 5B). However, in other studies the information about the stimulus was found to increase only slightly for longer integration times (Heller et al. 1995; Oram and Perrett 1992; Osborne et al. 2004; Tovee et al. 1993). The differences between studies are likely due to the specific temporal structure of the responses.

Noise correlation

Correlated noise in neural populations may result from various sources (review: Usrey and Reid 1999). It may be attributed to reciprocal synaptic connections between the neurons or might be the result of common synaptic input. For visual interneurons in the fly both sources are established: spikes in neurons with overlapping receptive fields are synchronized to a large extent, indicating that they are postsynaptic to the same input elements (Warzecha et al. 1998). Apart
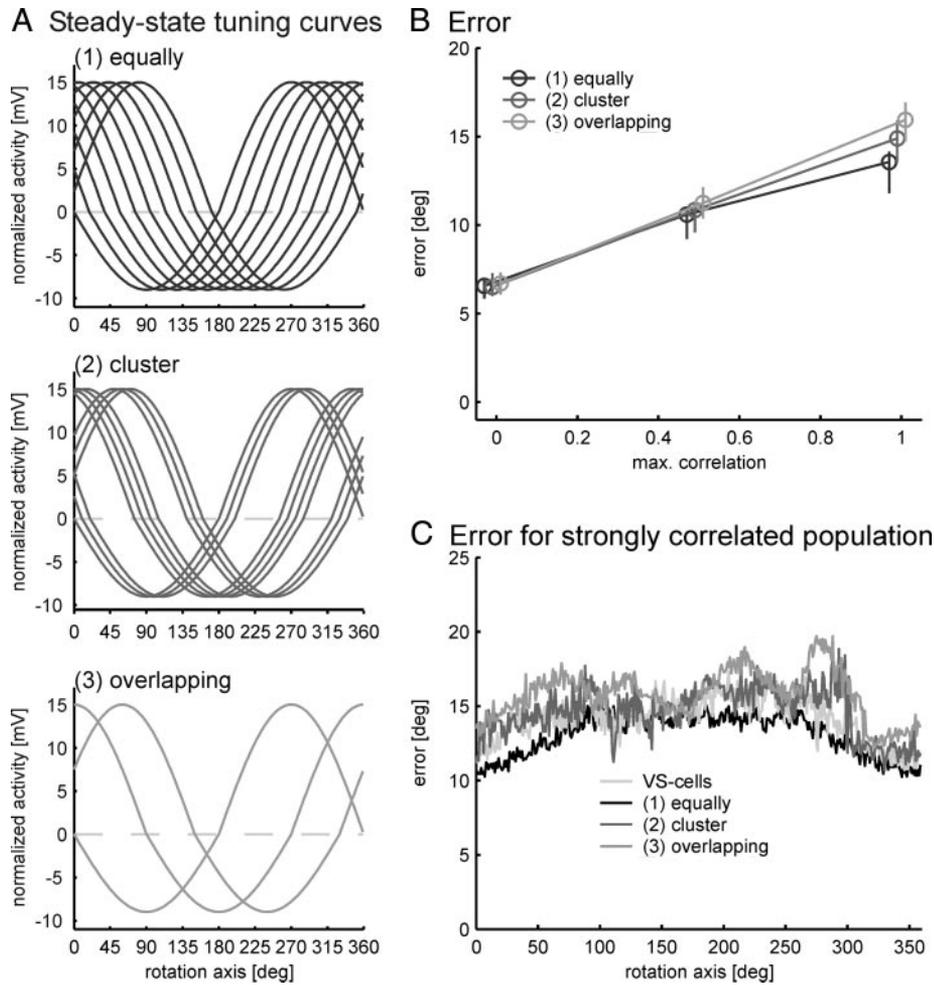
A Steady-state tuning curves

B Error

C Error for strongly correlated population

FIG. 9. Impact of the arrangement of tuning curves. *A*: steady-state tuning curves for the equally distributed (*1*), the clustered (*2*), and the overlapping population (*3*). *B*: decoding error for the 3 populations plotted as function of the correlation coefficient (correlation coefficient given for 2 neurons with identical tuning curves). *C*: decoding error for the strongly correlated populations and in addition, of the population with a distribution corresponding to the real VS neurons. The decoding error is obtained for an integration time of 10 ms after response onset.

from overlapping receptive fields neighboring VS neurons were recently found to be coupled via electrical synapses and to have partly correlated membrane potential fluctuations (Farrow et al. 2005; Haag and Borst 2004). Essentially, both experimental findings imply an increase of noise correlation with a decrease of the distance between the preferred stimulus axes of the neurons. Our results on population coding in VS neurons show that noise correlations slightly increase the decoding error. This result fits in with the results of theoretical studies predicting that distance-dependent noise correlations—often called local or limited-range correlations—deteriorate the performance of a population (Abbott and Dayan 1999; Wilke and Eurich 2002).

The impact of noise correlation on the ability of a neuronal population to encode information depends on the way in which noise is correlated and on the arrangement of the tuning curves of neurons (review: Averbeck and Lee 2004). In any case, correlation coefficients such as those measured in fly tangential neurons (Haag and Borst 2004; Warzecha et al. 1998) or those between retinal ganglion cells of vertebrates having overlapping receptive fields (e.g., Berry et al. 1997) have a relatively small effect on the decoding error.

Population size and spatial arrangement of neurons

Although two neurons with different preferred rotation axes should, in principle, be sufficient to encode any rotation axis of

the fly in the horizontal plane, the population of VS cells consists of 10 neurons. We found that the decoding error is small for a two-neuron population, but only if the neuronal response is integrated within a time window >20 ms or if the integration window starts some time after response onset. Whereas the number of VS cells is highly relevant when the rotation axis has to be estimated within a short time interval, the exact spatial arrangement of the VS neurons' preferred rotation axes has only a marginal effect on the decoding error. Our results revealed that the coding accuracy can be improved by different strategies: an ideal observer reading out the neural code may integrate the neuronal responses of a small population over a long time window or wait some time before starting the integration. Alternatively, the observer could take into account the responses of a larger population of neurons. The latter strategy allows for a fast reconstruction of the stimulus within a short integration time and seems to be used in the fly VS system. The relatively large population of VS neurons hints at the importance of fast processing of information to solve behavioral tasks, such as flight control and gaze stabilization.

The short integration times required to decode the rotation axis and the marginal effect of the spatial arrangement of preferred axes can be attributed partly to the graded response mode of VS neurons. Tuning curves of VS neurons do not rectify during motion about nonpreferred axes and thus each neuron contributes a distinct and different response to the

population activity for any rotation axis. For a population of neurons with rectified tuning curves, some stimuli will evoke subthreshold responses in the neurons that are affected by the rectification nonlinearity and lead to a "null" response (cf. Fig. 7*A*). To counteract the detrimental effect of "null" responses, the stimulus range evoking a "null" response would have to be reduced. This could be achieved by increasing the width of the tuning curves. Broadening of tuning curves, however, was shown to decrease the accuracy of a population code (e.g., Zhang and Sejnowski 1999; Zhang et al. 1998). Therefore given a certain width of the tuning curves, neurons with a graded response mode are superior to spiking neurons, especially for neuronal populations containing only a small number of elements. Neurons with a graded response mode may also be superior to spiking neurons if the integration times for decoding the neuronal responses is a limiting factor (for the consequences of the lengths of integration windows on graded and spiking neuronal responses, see also Kretzberg et al. 2001; Warzecha and Egelhaaf 2001).

Conclusion

We investigated the accuracy with which a population of visual interneurons in the fly encodes the information about the current self-motion from optic flow. Optic flow coding neurons have been found in many other species. Most of these neurons show broad and unimodal (single peaked) tuning to self-motion (e.g., Brosseau-Lachaine et al. 2001; Duffy and Wurtz 1991; Sherk et al. 1995; Tanaka and Saito 1989; Wylie and Frost 1999). One consequence of the broad tuning is that an individual neuron provides only ambiguous information about the actual self-motion or heading direction. Recent studies have shown that only the signals of a population of MST neurons provide reliable information about the heading direction (Ben Hamed et al. 2003; Lappe et al. 1996; Page and Duffy 2003). Current computational models of heading perception use the properties of the population of MT and MST neurons when trying to reproduce findings from human psychophysics (detailed review: Lappe 2000). All these studies corroborate the conclusion of the present study that only a population of neurons can provide unambiguous information about the current self-motion.

Our results indicate that a larger population of VS cells than the minimal number of two is important if the horizontal rotation axis has to be decoded from the population response of VS neurons with high accuracy within only 10 ms after response onset. Such short integration times match the time scale of natural self-motions of the fly. The most prominent feature of blowfly flight, fast head and body saccades as well as the intersaccadic intervals, take place on a time scale of some tens of milliseconds (van Hateren and Schilstra 1999). Hence the accuracy of the population of VS neurons in estimating horizontal rotations appears to be appropriate to extract behaviorally relevant information from the neuronal response under natural conditions. In a replay approach, developed to present visual stimuli the fly previously generated by its own behavior (Kern et al. 2005; van Hateren et al. 2005), we will test whether it is actually possible to reconstruct the animal's horizontal rotations from the population response under natural conditions as our current systems analysis approach suggests.

REFERENCES

Abbott LF and Dayan P. The effect of correlated variability on the accuracy of a population code. *Neural Comput* 11: 91–101, 1999.

Averbeck BB and Lee D. Coding and transmission of information by neural ensembles. *Trends Neurosci* 27: 225–30, 2004.

Azouz R and Gray CM. Cellular mechanisms contributing to response variability of cortical neurons in vivo. *J Neurosci* 19: 2209–2223, 1999.

Barberini CL, Horwitz GD, and Newsome WT. A comparison of spiking statistics in motion sensing neurons of flies and monkeys. In: *Computational, Neural and Ecological Constraints of Visual Motion Processing*, edited by Zanker JM and Zeil J. Heidelberg: Springer, 2001, p. 307–320.

Ben Hamed S, Page W, Duffy C, and Pouget A. MSTd neuronal basis functions for the population encoding of heading direction. *J Neurophysiol* 90: 549–58, 2003.

Berry MJ, Warland DK, and Meister M. The structure and precision of retinal spike trains. *Proc Natl Acad Sci USA* 94: 5411–5416, 1997.

Borst A and Haag J. Neural networks in the cockpit of the fly. *J Comp Physiol A* 188: 419–437, 2002.

Borst A, Reisenman C, and Haag J. Adaptation to response transients in fly motion vision. II. Model studies. *Vision Res* 43: 1309–1322, 2003.

Brosseau-Lachaine O, Faubert J, and Casanova C. Functional sub-regions for optic flow processing in the posteromedial lateral suprasylvian cortex of the cat. *Cereb Cortex* 11: 989–1001, 2001.

Dayan P and Abbott LF. *Theoretical Neuroscience: Computational and Mathematical Modeling of Neural Systems.* Cambridge, MA: MIT Press, 2001.

Duffy CJ and Wurtz RH. Sensitivity of MST neurons to optic flow stimuli. I. A continuum of response selectivity to large-field stimuli. *J Neurophysiol* 65: 1329–1345, 1991.

Egelhaaf M and Borst A. Transient and steady-state response properties of movement detectors. *J Opt Soc Am A* 6: 116–127, 1989.

Egelhaaf M and Borst A. Movement detection in arthropods. In: *Visual Motion and Its Role in the Stabilization of Gaze*, edited by Wallman J and Miles FA. Amsterdam: Elsevier, 1993, p. 53–77.

Egelhaaf M, Grewe J, Karmeier K, Kern R, Kurtz R, and Warzecha A. Novel approaches to visual information processing in insects: case studies on neuronal computations in the blowfly. In: *Methods in Insect Sensory Neuroscience*, edited by Christensen TA. Boca Raton, FL: CRC, 2004, p. 185–207.

Egelhaaf M, Kern R, Krapp HG, Kretzberg J, Kurtz R, and Warzecha AK. Neural encoding of behaviourally relevant visual-motion information in the fly. *Trends Neurosci* 25: 96–102, 2002.

Farrow K, Borst A, and Haag J. Sharing receptive fields with your neighbors: tuning the vertical system cells to wide field motion. *J Neurosci* 25: 3985–3993, 2005.

Földiak P. The "ideal homunculus": statistical inference from neural population responses. In: *Computation and Neural Systems*, edited by Eeckman F and Bower J. Norwell, MA: Kluwer Academic, 1993, p. 55–60.

Franceschini N. Sampling of visual environment by the compound eye of the fly: fundamentals and applications. In: *Photoreceptor Optics*, edited by Snyder AW and Menzel R. Berlin, Germany: Springer, 1975, p. 98–125.

Georgopoulos AP, Schwartz AB, and Kettner RE. Neuronal population coding of movement direction. *Science* 233: 1416–1419, 1986.

Gronenberg W, Milde JJ, and Strausfeld NJ. Oculomotor control in calliphorid flies: organization of descending neurons to neck motor neurons responding to visual stimuli. *J Comp Neurol* 361: 267–284, 1995.

Haag J and Borst A. Neural mechanism underlying complex receptive field properties of motion-sensitive interneurons. *Nat Neurosci* 7: 628–634, 2004.

Haag J and Borst A. Encoding of visual motion information and reliability in spiking and graded potential neurons. *J Neurosci* 17: 4809–4819, 1997.

Hausen K. Motion sensitive interneurons in the optomotor system of the fly. I. The horizontal cells: structure and signals. *Biol Cybern* 45: 143–156, 1982a.

Hausen K. Motion sensitive interneuron in the optomotor system of the fly. II. The horizontal cells: receptive field organization and response characteristics. *Biol Cybern* 46: 67–79, 1982b.

Hausen K and Egelhaaf M. Neural mechanisms of visual course control in insects,. In: *Facets of Vision*, edited by Stavenga DG and Hardie RC. Berlin, Heidelberg: Springer, 1989, 391–424.

Heller J, Hertz JA, Kjaer TW, and Richmond BJ. Information flow and temporal coding in primate pattern vision. *J Comput Neurosci* 2: 175–193, 1995.

Hengstenberg R. Spike responses of "non-spiking" visual interneurone. *Nature* 270: 338–340, 1977.

Hengstenberg R. Common visual response properties of giant vertical cells in the lobula plate of the blowfly calliphora. *J Comp Physiol [A]* 149: 179–193, 1982.

Hengstenberg R, Hausen K, and Hengstenberg B. The number and structure of giant vertical cells (VS) in the lobula plate of the blowfly *Calliphora erythrocephala*. *J Comp Physiol [A]* 149: 163–177, 1982.

Hinton GE, McClelland JL, and Rumelhart DE. Distributed representations. In: *Parallel Distributed Processing*, edited by Rumelhart DE, McClelland JL, and the PDP Research Group. Cambridge, MA: MIT Press, 1986.

Huston S and Krapp HG. The visual receptive field of a fly neck motor neuron. In: *Proceedings of the 29th Göttingen Neurobiology Conference*, edited by N. Elsner, Zimmermann H. Stuttgart: Thieme, 2003.

Johnston D and Wu M-S. *Foundations of Cellular Neurophysiology*, Cambridge, MA: MIT Press, 1995.

Karmeier K, Krapp HG, and Egelhaaf M. Robustness of the tuning of fly visual interneurons to rotatory optic flow. *J Neurophysiol* 90: 1626–34, 2003.

Kern R, van Hateren JH, Michaelis C, Lindemann J, and Egelhaaf M. Function of a fly motion sensitive neuron matches eye movements during free flight. *PLoS Biol* 3: e171, 2005.

Krapp HG. Neuronal matched filters for optic flow processing in flying insects. *Int Rev Neurobiol* 44: 93–120, 2000.

Krapp HG and Hengstenberg R. Estimation of self-motion by optic flow processing in single visual interneurons. *Nature* 384: 463–466, 1996.

Krapp HG, Hengstenberg B, and Hengstenberg R. Dendritic structure and receptive-field organization of optic flow processing interneurons in the fly. *J Neurophysiol* 79: 1902–1917, 1998.

Kretzberg J, Warzecha AK, and Egelhaaf M. Neural coding with graded membrane potential changes and spikes. *J Comput Neurosci.* 11: 153–164, 2001.

Lappe M. *Neuronal Processing of Optic Flow.* New York: Academic, 2000.

Lappe M, Bremmer F, Pekel M, Thiele A, and Hoffmann KP. Optic flow processing in monkey STS: a theoretical and experimental approach. *J Neurosci* 16: 6265–6285, 1996.

Lee D, Port NL, Kruse W, and Georgopoulos AP. Variability and correlated noise in the discharge of neurons in motor and parietal areas of the primate cortex. *J Neurosci* 18: 1161–1170, 1998.

Lindemann JP, Kern R, Michaelis C, Meyer P, van Hateren JH, and Egelhaaf M. FliMax, a novel stimulus device for panoramic and highspeed presentation of behaviorally generated optic flow. *Vision Res* 43: 779–791, 2003.

Lindemann JP, Kern R, van Hateren JH, Ritter H, and Egelhaaf M. On the computations analysing natural optic flow: quantitative model analysis of the blowfly motion vision pathway. *J Neurosci* 27: 6435–6448, 2005.

Miller JP, Jacobs GA, and Theunissen FE. Representation of sensory information in the cricket cercal sensory system. I. Response properties of the primary interneurons. *J Neurophysiol* 66: 1680–1689, 1991.

Nicolelis MA, Ghazanfar AA, Stambaugh CR, Oliveira LM, Laubach M, Chapin JK, Nelson RJ, and Kaas JH. Simultaneous encoding of tactile information by three primate cortical areas. *Nat Neurosci* 1: 621–30, 1998.

Oram MW, Foldiak P, Perrett DI, and Sengpiel F. The "Ideal Homunculus": decoding neural population signals. *Trends Neurosci* 21: 259–265, 1998.

Oram MW and Perrett DI. Time course of neural responses discriminating different views of the face and head. *J Neurophysiol* 68: 70–84, 1992.

Osborne LC, Bialek W, and Lisberger SG. Time course of information about motion direction in visual area MT of macaque monkeys. *J Neurosci* 24: 3210–3222, 2004.

Page WK and Duffy CJ. Heading representation in MST: sensory interactions and population encoding. *J Neurophysiol* 89: 1994–2013, 2003.

Pouget A, Deneve S, Ducom JC, and Latham PE. Narrow versus wide tuning curves: what's best for a population code? *Neural Comput* 11: 85–90, 1999.

Rolls ET, Treves A, and Tovee MJ. The representational capacity of the distributed encoding of information provided by populations of neurons in primate temporal visual cortex. *Exp Brain Res* 114: 149–162, 1997.

Salinas E and Abbott LF. Vector reconstruction from firing rates. *J Comput Neurosci* 1: 89–107, 1994.

Sanchez-Vives MV, Nowak LG, and McCormick DA. Cellular mechanisms of long-lasting adaptation in visual cortical neurons in vitro. *J Neurosci* 20: 4286–4299, 2000.

Sanger TD. Probability density estimation for the interpretation of neural population codes. *J Neurophysiol* 76: 2790–2793, 1996.

Schilstra C and van Hateren JH. Blowfly flight and optic flow. I. Thorax kinematics and flight dynamics. *J Exp Biol* 202: 1481–1490, 1999.

Sherk H, Kim JN, and Mulligan K. Are the preferred directions of neurons in cat extrastriate cortex related to optic flow? *Vis Neurosci* 12: 887–894, 1995.

Srinivasan MV. The impulse response of a movement-detecting neuron and its interpretation. *Vis Res* 23: 659–663, 1983.

Stavenga DG, Schwering PBW, and Tinbergen J. A three-compartment model describing temperature changes in thethered flying blowflies. *J Exp Biol* 185: 326–333, 1993.

Stemmann H, Freiwald WA, Wannig A, Schulzke E, and Eurich C. Encoding of dynamic visual stimuli by primate area MT neurons. *Neurocomputing* 65–66: 291–300, 2005.

Strausfeld NJ, Seyan H, and Milde JJ. The neck motor system of the fly *Calliphora erythrocephala*. I. Muscles and motor neurons. *J Comp Physiol [A]* 160: 205–224, 1987.

Tanaka K and Saito H. Analysis of motion of the visual field by direction, expansion/contraction, and rotation cells clustered in the dorsal part of the medial superior temporal area of the macaque monkey. *J Neurophysiol* 62: 626–641, 1989.

Theunissen FE and Miller JP. Representation of sensory information in the cricket cercal sensory system. II. Information theoretic calculation of system accuracy and optimal tuning-curve widths of four primary interneurons. *J Neurophysiol* 66: 1690–1703, 1991.

Tovee MJ, Rolls ET, Treves A, and Bellis RP. Information encoding and the responses of single neurons in the primate temporal visual cortex. *J Neurophysiol* 70: 640–654, 1993.

Usrey WM and Reid RC. Synchronous activity in the visual system. *Annu Rev Physiol* 61: 435–456, 1999.

van Hateren JH, Kern R, Schwerdtfeger G, and Egelhaaf M. Function and coding in the blowfly H1 neuron during naturalistic optic flow. *J Neurosci* 25: 4343–4352, 2005.

van Hateren JH and Schilstra C. Blowfly flight and optic flow. II. Head movements during flight. *J Exp Biol* 202: 1491–1500, 1999.

Warzecha A and Egelhaaf M. Neuronal encoding of visual motion in real-time. Heidelberg: Springer, 2001.

Warzecha AK, Egelhaaf M, and Borst A. Neural circuit tuning fly visual interneurons to motion of small objects. I. Dissection of the circuit by pharmacological and photoinactivation techniques. *J Neurophysiol* 69: 329–339, 1993.

Warzecha AK, Kretzberg J, and Egelhaaf M. Temporal precision of the encoding of motion information by visual interneurons. *Curr Biol* 8: 359–368, 1998.

Wilke SD and Eurich CW. Representational accuracy of stochastic neural populations. *Neural Comput* 14: 155–189, 2002.

Wylie DR and Frost BJ. Responses of neurons in the nucleus of the basal optic root to translational and rotational flowfields. *J Neurophysiol.* 81: 267–276, 1999.

Zhang K, Ginzburg I, McNaughton BL, and Sejnowski TJ. Interpreting neuronal population activity by reconstruction: unified framework with application to hippocampal place cells. *J Neurophysiol* 79: 1017–1044, 1998.

Zhang K and Sejnowski TJ. Neuronal tuning: To sharpen or broaden? *Neural Comput* 11: 75–84, 1999.

Zohary E, Shadlen MN, and Newsome WT. Correlated neuronal discharge rate and its implications for psychophysical performance. *Nature* 370: 140–143, 1994.